Regulation and Vibration Control of an FEM-Based Single-Link Flexible Arm Using Sliding-Mode Theory

YON-PING CHEN
HUAI-TE HSU
Department of Electrical and Control Engineering, National Chiao-Tung University, Hsinchu, Taiwan 300, Republic of China

(Received 24 November 1997; accepted 19 May 1999)

Abstract: Compared to the assumed-mode method (AMM), the finite-element method (FEM) is not only more applicable to the modeling of various kinds of flexible structures but also better in estimating the natural frequencies. Motivated from these features and modified from the work of Yeung and Chen for an AMM-based model, the sliding-mode controller introduced in this paper is developed to deal with the regulation problem and vibration suppression of an FEM-based single-link flexible arm. This paper will focus on the issue of how to change the FEM-based model into a form similar to the AMM-based model via the Schur decomposition. A technique to measure the well-estimated state variables required for the control is also presented. Finally, numerical simulation results are given to verify the robustness of the modified sliding-mode controller against payload variation.

Key Words: Flexible arm, FEM-based model, sliding mode, vibration control

1. INTRODUCTION

The mathematical model of a flexible structure can be approximately derived by using the assumed-mode method (AMM) or the finite-element method (FEM) (Junkins and Kim, 1993). Both methods have been widely applied to diverse applications (Bayo, 1987; Cannon and Schmitz, 1984; Chang and Chen, 1997; Matsuno, Murachi, and Sakawa, 1994; Yeung and Chen, 1989). It is recognized that the FEM is generally more applicable to the modeling of various kinds of flexible structures and usually also better in estimating the natural frequencies. Motivated by these features, this paper introduces a sliding-mode control for the FEM-based single-link flexible arm to treat vibration suppression.

The sliding-mode theory (Utkin, 1977; Itkis, 1976) is one of the important robust control theories. Recently, many investigators have paid attention to the sliding-mode control of the robotic flexible arm; for examples, see Yeung and Chen (1989) and Nathan and Singh (1991). In the work of Yeung and Chen (1989), the authors successfully developed a robust sliding-mode controller with respect to the payload variation for the AMM-based single-link flexible arm. Most significantly, they proposed a systematic scheme to choose the sliding function based on the AMM-based model. The determination of a sliding function is, however, an effort for conventional sliding-mode controller design. Therefore, to adopt their sliding-mode control appropriately, it is necessary to change the FEM-based model into a form similar to the AMM-based model. The main tool employed here is the Schur decomposition (Golub

Journal of Vibration and Control, 7: 741-752, 2001

and Van Loan, 1989) for the symmetric inertia and stiffness matrices. By using the Schur decomposition, the FEM-based model is decomposed into two subsystems: one is for the lower natural frequencies and the other for the higher natural frequencies. Since only the lower natural frequencies are well estimated, the FEM-based model is further reduced by neglecting all the terms related to the higher natural frequencies. Most important, such a reduced FEM-based model is expressed in a similar fashion to the AMM-based model. Therefore, its sliding-mode controller design can be developed by modifying the work proposed by Yeung and Chen (1989) for the AMM-based model. Furthermore, n strain gauges are required to obtain the variables for the FEM-based control input when the flexible arm is considered to possess n equal-length segments. Note that the number of the strain gauges is the same as that needed for an n-mode AMM-based model.

The next section will derive the reduced FEM-based model. In Section 3, a modified sliding-mode controller is developed to deal with vibration suppression. The robustness to the payload variation of the sliding-mode control will be illustrated by simulation results shown in Section 4. Finally, the concluding remarks are given in Section 5.

2. REDUCED FEM-BASED MODEL OF A SINGLE FLEXIBLE ARM

Based on the finite element method (Junkins and Kim, 1993), the dynamic equations of a single-link flexible arm moving in a horizontal plane, shown in Figure 1, can be derived in a straightforward manner. First, the flexible arm is assumed to possess n equal-length segments with a concentrated payload m_t at the tip position. Further define v_1^i and v_2^i as the bending deflection and slope of the ith segment at the right end. Then, by using Hamilton's principle, the FEM-based dynamic equations of a single flexible arm can be derived as

$$\begin{bmatrix} \mathbf{m}_{\theta\theta}(m_t) & \mathbf{m}_{\theta v}^T(m_t) \\ \mathbf{m}_{\theta v}(m_t) & \mathbf{M}_{vv}(m_t) \end{bmatrix} \begin{bmatrix} \ddot{\boldsymbol{\theta}} \\ \ddot{\mathbf{v}} \end{bmatrix} + \begin{bmatrix} 0 & \mathbf{0}^T \\ \mathbf{0} & \mathbf{K}_{vv} \end{bmatrix} \begin{bmatrix} \boldsymbol{\theta} \\ \mathbf{v} \end{bmatrix} = \begin{bmatrix} 1 \\ \mathbf{0} \end{bmatrix} u, \qquad (1)$$

where θ is the rotor's angular position and u represents the control torque and bending variables $\mathbf{v} = [v_1^1\, v_2^1\, v_1^2\, v_2^2\, \ldots\, v_1^n\, v_2^n]^T$. It is noticed that $\{\mathbf{m}_{\theta\theta}, \mathbf{m}_{\theta v}, \mathbf{M}_{vv}\}$ are all functions of m_t and $\left\{\mathbf{M}_{vv}, \mathbf{K}_{vv} \begin{bmatrix} \mathbf{m}_{\theta\theta} & \mathbf{m}_{\theta v}^T \\ \mathbf{m}_{\theta v} & \mathbf{M}_{vv} \end{bmatrix}\right\}$ are all symmetric positive-definite matrices. For convenience, when a variable is related to the payload m_t or the ith segment, $1 \leq i \leq n$, it will be denoted with a superscript t or i. The payload m_t is uncertain, bounded between $m_t^{\min}$ and $m_t^{\max}$, with a nominal value m_t^o $(\in [m_t^{\min}, m_t^{\max}])$.

Since v possesses $2n$ variables, $2n$ natural frequencies will result from (1). By using the Schur decomposition (Golub and Van Loan, 1989), the symmetric positive-definite matrix $\mathbf{M}_{vv}$ can be expressed as

$$\mathbf{M}_{vv} = \mathbf{U}^T \boldsymbol{\Lambda} \mathbf{U} = \mathbf{N}^T \mathbf{N}, \qquad (2)$$

where $\mathbf{U}$ is an orthogonal matrix, $\boldsymbol{\Lambda}$ is a positive diagonal matrix, and $\mathbf{N} = \boldsymbol{\Lambda}^{1/2}\mathbf{U}$. Let $\mathbf{K}_{vN} = \mathbf{N}^{-T}\mathbf{K}_{vv}\mathbf{N}^{-1}$, which is also symmetric positive-definite. Once again, by using the Schur decomposition, we have $\mathbf{K}_{vN} = \mathbf{P}^T \boldsymbol{\Omega} \mathbf{P}$, where $\mathbf{P}$ is an orthogonal matrix and $\boldsymbol{\Omega}$ is a positive diagonal matrix. Hence,

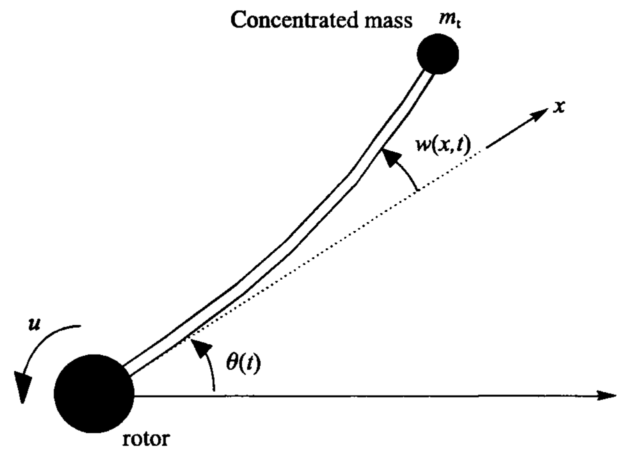

Figure 1. Single-link flexible arm.

$$\mathbf{K}_{vv} = \mathbf{L}^T \boldsymbol{\Omega} \mathbf{L}, \tag{3}$$

where $\mathbf{L} = \mathbf{PN}$. Note that all the matrices $\boldsymbol{\Lambda}$, $\boldsymbol{\Omega}$, $\mathbf{N}$, $\mathbf{P}$, and $\mathbf{L}$ depend on the payload m_t. Since $\mathbf{P}$ is orthogonal, that is, $\mathbf{P}^T\mathbf{P} = \mathbf{I}$, from (2) it can be obtained that

$$\mathbf{M}_{vv} = \mathbf{N}^T\mathbf{P}^T\mathbf{P}\mathbf{N} = \mathbf{L}^T\mathbf{L}. \tag{4}$$

Let $\mathbf{y} = \mathbf{Lv} = [y_1 \ \dots \ y_{2n}]^T$, then (1) can be rewritten as

$$\begin{bmatrix} \mathbf{m}_{\theta\theta}(m_t) & \mathbf{b}^T(m_t) \\ \mathbf{b}(m_t) & \mathbf{I} \end{bmatrix} \begin{bmatrix} \ddot{\boldsymbol{\theta}} \\ \ddot{\mathbf{y}} \end{bmatrix} + \begin{bmatrix} 0 & \mathbf{0} \\ \mathbf{0} & \boldsymbol{\Omega}(m_t) \end{bmatrix} \begin{bmatrix} \boldsymbol{\theta} \\ \mathbf{y} \end{bmatrix} = \begin{bmatrix} 1 \\ \mathbf{0} \end{bmatrix} u, \tag{5}$$

where $\mathbf{b}(m_t) = \mathbf{L}^{-T}\mathbf{m}_{\theta v}$. Clearly, in case that $\ddot{\boldsymbol{\theta}} = 0$, a vibration motion can be deduced from (5) as below:

$$\ddot{\mathbf{y}} + \boldsymbol{\Omega}(m_t)\mathbf{y} = \mathbf{0}. \tag{6}$$

Without loss of generality, let $\boldsymbol{\Omega}(m_t)$be

$$\boldsymbol{\Omega}(m_t) = \begin{bmatrix} \omega_1^2 & & & \mathbf{0} \\ & \omega_2^2 & & \\ & & \ddots & \\ \mathbf{0} & & & \omega_{2n}^2 \end{bmatrix},$$

with $\omega_1 < \omega_2 < \ldots < \omega_{2n}$. This means the FEM-based model possesses $2n$ natural frequencies from ω_1 to ω_{2n}. It is known that the lower n natural frequencies of a flexible arm are well estimated by ω_1 to ω_n. However, unlike ω_1 to ω_n, the higher frequencies ω_{n+1} to ω_{2n} do not correspond to any physical natural frequencies. An approximate FEM-based model is usually obtained by neglecting all the components related to these higher frequencies ω_{n+1} to ω_{2n}. Such approximation is conceivable since the accumulated energy of frequencies higher than ω_n is generally much smaller than that of lower frequencies from ω_1 to ω_n. Besides, to further make the approximate model more precise, the number of nature modes n is often carefully selected so as not to excite any component with frequency higher than ω_n via the applied control input. Now the FEM-based model (5) is reduced as

$$\begin{bmatrix} \mathbf{m}_{\theta\theta}(m_t) & \bar{\mathbf{b}}^T(m_t) \\ \bar{\mathbf{b}}(m_t) & \bar{\mathbf{I}} \end{bmatrix} \begin{bmatrix} \ddot{\theta} \\ \ddot{\bar{\mathbf{y}}} \end{bmatrix} + \begin{bmatrix} 0 & \bar{\mathbf{0}} \\ \bar{\mathbf{0}} & \bar{\Omega}(m_t) \end{bmatrix} \begin{bmatrix} \theta \\ \bar{\mathbf{y}} \end{bmatrix} = \begin{bmatrix} 1 \\ \bar{\mathbf{0}} \end{bmatrix} u, \tag{7}$$

where $\bar{\mathbf{y}} = [y_1 \ldots y_n]^T$. Here, all the variables of $\mathbf{y}_h = [y_{n+1} \ldots y_{2n}]^T$, related to ω_{n+1} to ω_{2n}, are eliminated. It is important to point out that the reduced model (7) is similar to the AMM-based model shown in the work of Yeung and Chen (1989) and, hence, the sliding-mode controller developed for (7) will be a modified version of the controller proposed by them.

Under the variation of m_t ($\in [m_t^{\min}, m_t^{\max}]$), the control objective is to robustly regulate the angular position θ to a specified value θ_d without any vibration. Before the controller design, the main task is to obtain the variables $\bar{\mathbf{y}} = [y_1 \ldots y_n]^T$ required for the control algorithm. Strain gauges are used as the sensors. Each segment along the flexible arm is instrumented with one strain gauge, and then n strain values are measured to be $\mathbf{z} = [z_1\, z_2 \ldots z_n]^T$. These quantities can be related to bending variables v as $\mathbf{z} = \mathbf{G}\mathbf{v}$ with $\mathbf{G} \in R^{n\times 2n}$. Since $\mathbf{y} = \mathbf{L}\mathbf{v}$, we have $\mathbf{z} = \Gamma\mathbf{y}$ with $\Gamma = \mathbf{G}\mathbf{L}^{-1}$. It can be further expressed by $\mathbf{z} = \Gamma_1\bar{\mathbf{y}} + \Gamma_2\mathbf{y}_h$, where Γ_1 ($\in R^{n\times n}$) is assumed nonsingular. The neglect of $\mathbf{y}_h$ yields $\mathbf{z} \approx \Gamma_1\bar{\mathbf{y}}$, that is, the required $\bar{\mathbf{y}}$ can be obtained as

$$\bar{\mathbf{y}} \approx \Gamma_1^{-1}\mathbf{z}. \tag{8}$$

Unfortunately, $\bar{\mathbf{y}}$ is still not achievable from (8) due to the fact that $\Gamma_1 \equiv \Gamma_1(m_t)$, depending on the uncertain payload m_t. To solve such a problem, an intuitive way is to make the nominal approximation

$$\bar{\mathbf{y}}^o \equiv \bar{\mathbf{y}}(m_t^o) = \Gamma_1^{-1}(m_t^o)\,\mathbf{z}. \tag{9}$$

Evidently, there exists an unknown deviation $\bar{\mathbf{y}} - \bar{\mathbf{y}}^o$, which should be carefully handled in the controller design. Next, we develop the sliding-mode controller for the reduced FEM-based model (7).

3. SLIDING-MODE CONTROLLER DESIGN

The reduced model (7) can be rewritten into the following form:

$$\mathbf{m}_{\theta\theta}(m_t)\ddot{\theta} + \bar{\mathbf{b}}^T(m_t)\ddot{\bar{\mathbf{y}}} = u \tag{10}$$

$$\bar{\mathbf{b}}(m_t)\ddot{\theta} + \ddot{\bar{\mathbf{y}}} + \bar{\boldsymbol{\Omega}}(m_t)\bar{\mathbf{y}} = \bar{\mathbf{0}}. \tag{11}$$

Under the uncertain payload m_t, the control objective is to robustly regulate the angular position θ to a specified value θ_d without any vibration, that is, $\theta - \theta_d = 0$ and $\bar{\mathbf{y}} = \bar{\mathbf{0}}$. Define $e = \theta - \theta_d$, then (10) and (11) are rearranged as

$$\mathbf{m}_{\theta\theta}(m_t)\ddot{e} + \bar{\mathbf{b}}^T(m_t)\ddot{\bar{\mathbf{y}}} = u \tag{12}$$

$$\bar{\mathbf{b}}(m_t)\ddot{e} + \ddot{\bar{\mathbf{y}}} + \bar{\boldsymbol{\Omega}}(m_t)\bar{\mathbf{y}} = \mathbf{0}. \tag{13}$$

In general, there are two basic steps for the sliding-mode controller design. First, the sliding variable is selected such that the system is stabilized in the sliding mode. Second, the control algorithm is designed to satisfy the sliding condition.

In the first step, the sliding variable is chosen to be

$$s = \dot{e} + ce + c' \int e \,\mathrm{dt} + \mathbf{a}^T\bar{\mathbf{y}}^o + \mathbf{a}'^T \int \bar{\mathbf{y}}^o \mathrm{dt}, \tag{14}$$

where $c, c', \mathbf{a}^T = [a_1\ a_2\ \ldots\ a_n]$, and $\mathbf{a}'^T = [a_1'\ a_2'\ \ldots\ a_n']$ are all constant and will be determined by the pole-placement method. Since $\bar{\mathbf{y}}^o = \Gamma_1^{-1}(m_t^o)\mathbf{z}$ and $\bar{\mathbf{y}} = \Gamma_1^{-1}(m_t)\mathbf{z}$, we have

$$\bar{\mathbf{y}}^o = \mathbf{Q}(m_t)\bar{\mathbf{y}}, \tag{15}$$

where $\mathbf{Q}(m_t) = \Gamma_1^{-1}(m_t^o)\Gamma_1(m_t)$ and $\mathbf{Q}(m_t^o) = \mathbf{I}$. Assume that the system is successfully controlled to perform the sliding motion $s = 0$. From the concept of equivalent control (Utkin, 1977), it can be obtained that $\dot{s} = 0$ as the equivalent control is applied to the system. Therefore, differentiating (14) yields

$$\dot{s} = \ddot{e} + c\dot{e} + c'e + \mathbf{a}^T\mathbf{Q}(m_t)\dot{\bar{\mathbf{y}}} + \mathbf{a}'^T\mathbf{Q}(m_t)\bar{\mathbf{y}} = 0. \tag{16}$$

Now, the system in the sliding mode can be described by (16) and (13). Note that (12) has been replaced by (16). Further taking the Laplace transform of (16) and (13) results in

$$\begin{bmatrix} \lambda^2+\lambda c+c' & (\lambda \mathbf{a}^T+\mathbf{a}'^T)\,\mathbf{Q}(m_t) \\ \lambda^2\bar{\mathbf{b}}(m_t) & \lambda^2\bar{\mathbf{I}}+\bar{\mathbf{\Omega}}(m_t) \end{bmatrix} \begin{bmatrix} E \\ \bar{\mathbf{Y}} \end{bmatrix} = \begin{bmatrix} 0 \\ \mathbf{0} \end{bmatrix}, \tag{17}$$

where E and $\bar{\mathbf{Y}}$ are the Laplace transforms of e and $\bar{\mathbf{y}}$, respectively. It can be found that the characteristic equation of (17) is expressed by

$$\begin{vmatrix} \lambda^2+\lambda c+c' & (\lambda \mathbf{a}^T+\mathbf{a}'^T)\,\mathbf{Q}(m_t) \\ \lambda^2\bar{\mathbf{b}}(m_t) & \lambda^2\bar{\mathbf{I}}+\bar{\mathbf{\Omega}}(m_t) \end{vmatrix} = 0, \tag{18}$$

where the coefficients $c, c', \mathbf{a}$, and $\mathbf{a}'$ are commonly determined by the pole-placement method. Unfortunately, the uncertain payload m_t makes it more complicated. In this paper, the pole-placement method is adopted only for the nominal case $m_t = m_t^o$, where the characteristic equation (18) can be written as

$$\begin{vmatrix} \lambda^2+c\lambda+c' & a_1\lambda+a_1' & a_2\lambda+a_2' & \cdots & a_2\lambda+a_n' \\ \lambda^2 b_1(m_t^o) & \lambda^2+\omega_1^2(m_t^o) & 0 & \cdots & 0 \\ \lambda^2 b_2(m_t^o) & 0 & \lambda^2+\omega_2^2(m_t^o) & \cdots & 0 \\ \vdots & \vdots & \vdots & \ddots & \vdots \\ \lambda^2 b_n(m_t^o) & 0 & 0 & \cdots & \lambda^2+\omega_n^2(m_t^o) \end{vmatrix} = 0. \tag{19}$$

Note that $\mathbf{Q}(m_t^o) = \mathbf{I}$. According to the work by Yeung and Chen (1989), the $2n+2$ coefficients $\{c, c', a_1, a_1', \ldots, a_n, a_n'\}$ in (19) are uniquely determined by assigning $2n+2$ stable eigenvalues. In fact, these stable eigenvalues should be carefully assigned such that with the coefficients obtained from the nominal case, the characteristic equation (18) must also possess stable eigenvalues for all $m_t \in [m_t^{\min}, m_t^{\max}]$. If so, the robust feature against the payload variation is guaranteed. A rule of thumb to choose the appropriate stable eigenvalues for the single-link flexible arm was also shown in the work of Yeung and Chen (1989). This paper will adopt their suggestion and demonstrate it in the next section.

Once the coefficients $\{c, c', a_1, a_1', \ldots, a_n, a_n'\}$ in the sliding variable (14) are determined, the first step of the controller design is completed. The second step is to develop the control algorithm to satisfy the sliding condition. From (12) and (13), it can be obtained that

$$\Delta\ddot{e} - \bar{\mathbf{b}}^T\bar{\mathbf{\Omega}}\bar{\mathbf{y}} = u, \tag{20}$$

where $\Delta = \mathbf{m}_{\theta\theta} - \bar{\mathbf{b}}^T\bar{\mathbf{b}}$. Since $\Delta > \mathbf{m}_{\theta\theta} - \mathbf{b}^T\mathbf{b} = \mathbf{m}_{\theta\theta} - \mathbf{m}_{\theta v}^T\mathbf{M}_{vv}^{-1}\mathbf{m}_{\theta v} > 0$, the candidate of Lyapunov function can be given as

$$V = \frac{1}{2}\Delta s^2 \geq 0, \tag{21}$$

where the equality is true only for $s = 0$. From (14), differentiating (21) yields

$$\dot{V} = \Delta\ddot{e}s + \Delta\tau s, \tag{22}$$

where $\tau = c\dot{e} + c'e + \mathbf{a}^T \dot{\bar{\mathbf{y}}}^o + \mathbf{a}'^T \bar{\mathbf{y}}^o$. It can be further rearranged from (8) and (20) as

$$\dot{V} = us + \left(\mathbf{w}^T \mathbf{z} + \triangle\tau\right) s, \tag{23}$$

where $\mathbf{w}^T = \bar{\mathbf{b}}^T \bar{\mathbf{\Omega}} \mathbf{\Gamma}_1^{-1}$. Since $\mathbf{w} \equiv \mathbf{w}(m_t), \Delta \equiv \Delta(m_t)$, and $m_t \in [m_t^{\min}, m_t^{\max}]$, we assume that

$$\begin{aligned} \mathbf{w}(m_t) &= \mathbf{w}(m_t^o) + \widetilde{\mathbf{w}}(m_t), \qquad \|\widetilde{w}_i(m_t)\| \le \widetilde{w}_{i,\max} \\ \triangle(m_t) &= \triangle(m_t^o) + \widetilde{\triangle}(m_t), \qquad \left\|\widetilde{\triangle}(m_t)\right\| \le \widetilde{\triangle}_{\max}. \end{aligned} \tag{24}$$

Let the control law be

$$u = -\left(\mathbf{w}^T(m_t^o)\mathbf{z} + \triangle(m_t^o)\tau\right) - \left(\sum_{i=1}^{n} \widetilde{w}_{i,\max}|z_i| + \widetilde{\triangle}_{\max}|\tau|\right)\operatorname{sgn}(s), \tag{25}$$

then

$$\dot{V} = -|s| \cdot \left\{\sum_{i=1}^{n} (\widetilde{w}_{i,\max}|z_i| - \widetilde{w}_i z_i \operatorname{sgn}(s)) + (\widetilde{\triangle}_{\max}|\tau| - \widetilde{\triangle}\tau\operatorname{sgn}(s))\right\} \le 0, \tag{26}$$

where the equality is true only for $s = 0$. Therefore, V is a Lyapunov function and the system will be driven to the sliding mode $s = 0$, as desired.

In practice, the implementation of $\operatorname{sgn}(s)$often generates undesirable high-frequency chattering and degrades the system performance. To smooth out the chattering, the control law is changed into

$$u = -\left(\mathbf{w}^T(m_t^o)\mathbf{z} + \triangle(m_t^o)\tau\right) - \left(\sum_{i=1}^{n} \widetilde{w}_{i,\max} z_i + \widetilde{\triangle}_{\max}|\tau|\right)\operatorname{sat}(s,\varepsilon), \tag{27}$$

where

$$\operatorname{sat}(s,\varepsilon) = \begin{cases} \operatorname{sgn}(s) & |s| > \varepsilon \\ s/\varepsilon & |s| \le \varepsilon \end{cases}$$

is used to replace $\operatorname{sgn}(s)$. As a consequence, the system is no longer restricted to the infinitesimal sliding mode $s = 0$ but constrained in the sliding layer $| s | \le \varepsilon$ with thickness ε. This completes the sliding-mode controller design.

One other important phenomenon should be addressed here before getting into the numerical simulation. It is noticed that the control algorithm is derived only for the reduced model, expressed by (12) and (13), without considering those high-frequency components.

They are treated as the unmodeled terms and always exist in the practical systems. In the next section, although the controller is designed based on the reduced model, the simulation is implemented for the original system (1), possessing the high-frequency components. As a result, the simulation results will show that the system performance is badly affected when the control law excites these unmodeled high-frequency components. This is especially true for the system transient behavior before reaching the desired set-point.

4. NUMERICAL SIMULATION

As a demonstration, we will carry out a numerical simulation for a single-link flexible arm, which has a uniformly distributed mass m along the central axis and a rectangular cross-sectional area. The structural parameters are listed as below:

- mass of the beam $m = 0.332$ kg
- length of the beam $l = 0.950$ m
- rectangular cross-sectional area $A = 4.176 \times 10^{-5}$ m^2
- mass per unit length $\rho = 0.3495$ kg/m
- Young's modulus $E = 2.095 \times 10^{11}$ Nt/m^2
- payload $m_t \in [0.3, 0.5]$ kg
- nominal payload $m_t^o = 0.4$ kg

If the flexible arm is considered to possess 3 equal-length segments, then according to the finite-element method, the dynamic equations will be derived as (1) with the bending variables $\mathbf{v} = [v_1^1\ v_2^1\ v_1^2\ v_2^2\ v_1^3\ v_2^3]^T$. By the Schur decomposition, the bending variables are transformed as $\mathbf{y} = \mathbf{L}\mathbf{v} = [y_1\ \ldots\ y_6]^T$ and the dynamic equations are changed into (5), which contains 6 natural frequencies ω_1 to ω_6 and $\omega_1 < \omega_2 < \ldots < \omega_6$. Note that the natural frequency ω_i is related to the variable y_i, for $i = 1, 2, \ldots, 6$. Since only the lower natural frequencies $\omega_1 = 3.585, \omega_2 = 22.973$, and $\omega_3 = 57.097$ are well estimated, the dynamic equations are reduced to (7) with $\bar{\mathbf{y}} = [y_1\ y_2\ y_3]^T$. From (8), $\bar{\mathbf{y}} \approx \Gamma_1^{-1}\mathbf{z}$, where $\mathbf{z} = [z_1\ z_2\ z_3]^T$ are measured by three strain gauges. The ith strain gauge is located at the middle position of the ith segment.

Under the variation of payload m_t, the control objective is to robustly regulate the angular position θ to a specified value $\theta_d = \pi/2$ without any vibration. Define the error function as $e = \theta - \theta_d$. Then, in the first step of the controller design, the sliding variable is chosen as

$$s = \dot{e} + ce + c' \int e\,\mathrm{dt} + \mathbf{a}^T \bar{\mathbf{y}}^o + \mathbf{a}'^T \int \bar{\mathbf{y}}^o \mathrm{dt}, \tag{28}$$

where the coefficients $c, c', \mathbf{a}^T = [a_1\ a_2\ a_3]$ and $\mathbf{a}'^T = [a_1'\ a_2'\ a_3']$ are all constant and determined by assigning the roots of (19) with

$$\left\{-1, -2, -3.585\frac{1 \pm j}{\sqrt{2}}, -22.973\frac{1 \pm j}{\sqrt{2}}, -57.097\frac{1 \pm j}{\sqrt{2}}\right\}. \tag{29}$$

It should be emphasized here that if these roots are sensitive to the variation of payload, the sliding-mode controller might be only suitable for a small region of m_t around the nominal value m_t^o. According to the suggestion by Yeung and Chen (1989), the ith pair of complex roots in (29) are located at the angles $\pm 135°$ on the complex plane with a magnitude ω_i. Later, from the simulation results, it will be found that the robust feature against the payload variation is achieved by using the eigenvalues in (29).

After the sliding variable is determined, the next step is to design the control algorithm for the sliding condition. Following the design procedure, the control law (27) becomes

$$u = -\left(\mathbf{w}^T(m_t^o)\mathbf{z} + \triangle(m_t^o)\tau\right) - \left(\sum\nolimits_{i=1}^{n} \widetilde{w}_{i,\max}|z_i| + \widetilde{\triangle}_{\max}|\tau|\right)\mathrm{sat}(s,\varepsilon), \tag{30}$$

where

$$\begin{aligned} \mathbf{w}(m_t^o) &= [75.28 \quad -28.07 \quad 37.20]^T, \quad \triangle(m_t^o) = 0.0062,\ \widetilde{w}_{1,\max} = 0.017, \\ \widetilde{w}_{2,\max} &= 0.0033,\ \widetilde{w}_{3,\max} = 0.0187,\ \widetilde{\triangle}_{\max} = 0.0011,\ \varepsilon = 0.01. \end{aligned}$$

As mentioned before, the use of $\mathrm{sat}(s,\varepsilon)$ is to ameliorate the chattering problem. To demonstrate the robustness of the control law, numerical simulation is implemented on the original model (1), containing all the neglected terms. In addition, three cases of $m_t = 0.3, m_t = m_t^o = 0.4$, and $m_t = 0.5$ are considered for payload variation. Figures 2 through 4 show the simulation results. In Figure 2, although the control algorithm is designed for the nominal case $m_t = 0.4$, the tip-position is still successfully controlled to the desired position for the other two cases $m_t = 0.3, 0.5$. Clearly, this verifies that the sliding-mode control is robust to the payload variation. Figure 3 shows the required control inputs for these three cases, where chattering still exists during the transient $0 < t < 2$. It seems that the use of saturation function cannot avoid the chattering problem. In fact, such chattering is caused by those unmodeled terms in (1) related to ω_4 to ω_6, which have been included in the simulation. They, of course, cannot be effectively handled by the control algorithm (30), which is only derived to deal with the reduced model (12) and (13). Such defect can be also seen from Figure 4, which presents the sliding function for $m_t = 0.4$. During the transient $0 < t < 2$, the system trajectory is not completely constrained in the sliding layer $| s | \leq \varepsilon (= 0.01)$. It is because the system tends to reach the control goal as fast as possible from the starting time. As a result, the control input requires high-frequency components to speed up the system response during the transient. Simultaneously, the high-frequency unmodeled terms are also stimulated to degrade the system response. After the transient, the system is well controlled to the neighborhood of the control goal. That means the control input intends to drive the system to the destination smoothly; therefore, the high-frequency unmodeled terms will not be excited. As expected, the system is controlled without any chattering after the transient.

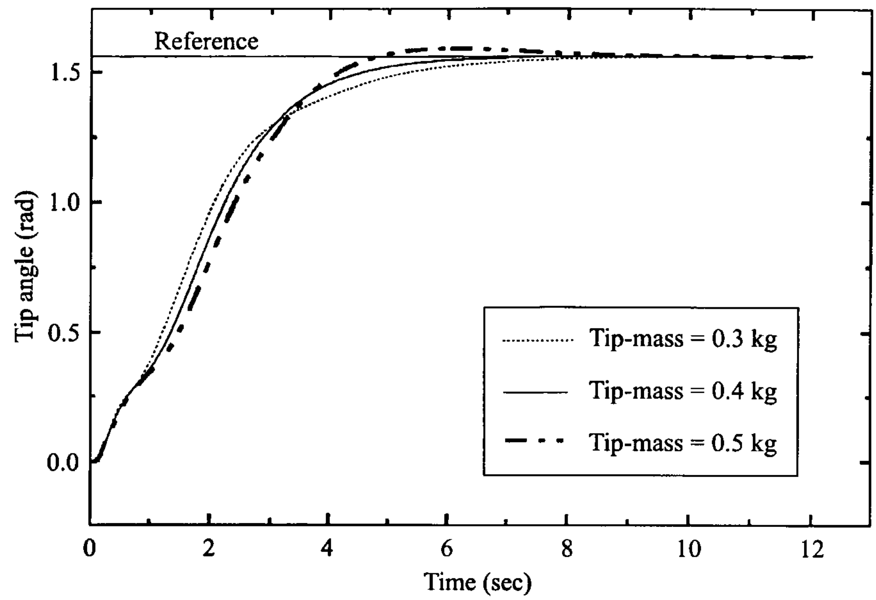

Figure 2. Tip angle for the cases of $m_t = 0.3, 0.4, 0.5$ kg.

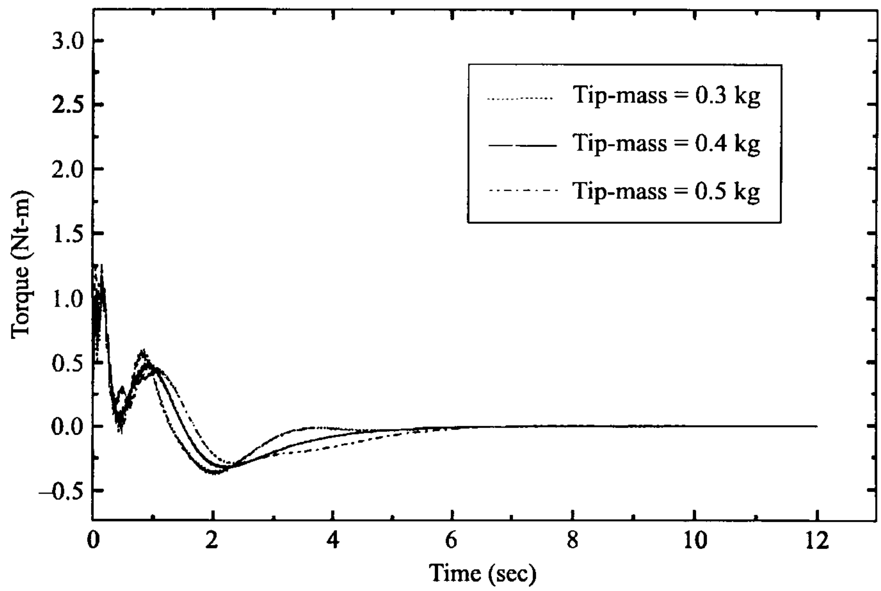

Figure 3. Control input for the three cases $m_t = 0.3, 0.4, 0.5$ kg.

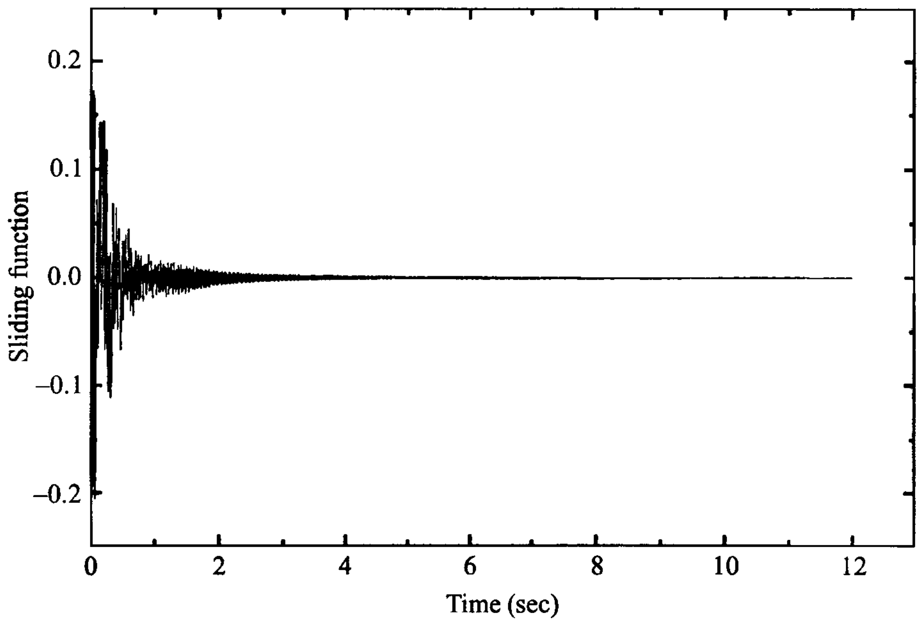

Figure 4. Sliding variable for $m_t = 0.4$ kg.

5. CONCLUSION

This paper develops a sliding-mode control of an FEM-based single-link flexible arm. Before the controller design, the FEM-based model is reduced via the Schur decomposition to keep only the lower half of natural frequencies, which are well estimated in the FEM-based model. Simulation results are included to illustrate the robustness of the sliding-mode control against the payload variation.

Acknowledgment. Research was supported by National Science Council, Taiwan, R.O.C., under Contract NSC 86-2213-E-009-056.

REFERENCES

Bayo, E., 1987, "A finite-element approach to control the end-point motion of a single-link flexible robot," *Journal of Robotic Systems* 4(1), 63-75.

Cannon, R. and Schmitz, E., 1984, "Initial experiments on end-point control of a flexible one-link robot," *International Journal of Robotics* 3(3), 62-75.

Chang, J. L. and Chen, Y. P., 1997, "Force control of a single-link flexible arm using sliding-mode theory," *Journal of Vibration and Control* 3(4), 439-452.

Golub, G. H. and Van Loan, C. F., 1989, *Matrix Computations*, Johns Hopkins University Press, London.

Itkis, U., 1976, *Control System of Variable Structure*, John Wiley, New York.

Junkins, J. L. and Kim, Y., 1993, *Introduction to Dynamics and Control of Flexible Structure*, AIAA, Washington, DC.

Matsuno, F., Murachi, T., and Sakawa, Y., 1994, "Feedback control of decoupled bending and torsional vibrations of flexible beams," *Journal of Robotic Systems* **11**(5), 341-353.

Nathan, P. J. and Singh, S. N., 1991, "Sliding-mode control and elastic mode stabilization of a robotic arm with flexible links," *Journal of Dynamic System, Measurement, and Control* **113**, 669-676.

Utkin, V. I., 1977, "Variable structure systems with sliding mode: A survey," *IEEE Transactions on Automatic Control* **22**, 212-222.

Yeung, K. S. and Chen, Y. P., 1989, "Regulation of a one-link flexible robot arm using sliding-mode technique," *International Journal of Control* **49**, 1965-1978.